Journal of Mathematical Chemistry Vol. 36, No. 4, August 2004 (© 2004)

Spiroconjugation in 1-, 2-, and 3-dimensions: The foundations of a spiro quantum chemistry

Michael J. Bucknum

Department of Chemistry and Chemical Biology, Baker Laboratory, Cornell University, Ithaca, NY 14853, USA

Eduardo A. Castro*

INIFTA, Theoretical Chemistry Division, Faculty of Exact Sciences, Chemistry Department, La Plata University, Diag. 113 y 64, Suc. 4, C.C. 16, La Plata 1900, Argentina
E-mail: castro@quimica.unlp.edu.ar/jubert@arnet.com.ar

Received 20 May 2004; revised 29 June 2004

A recent paper has described the structure of a hypothetical 3-,4-connected net termed glitter. This is a model of an allotrope of carbon in the form of a synthetic metal. That paper pointed to the importance of through-space p_σ interactions of adjacent olefin units in the net in understanding the electronic structure at the Fermi level. The present communication elucidates the role of spiroconjugation in understanding features of the electronic band structure and density of states of glitter. With this analysis of spiroconjugation in the 1-dimensional polyspiroquinoid polymer and the 3-dimensional glitter lattice, the foundations have been laid for a new type of quantum chemistry herein called spiro quantum chemistry. Spiro quantum chemistry complements traditional quantum chemistry which is focused on linear polyenes, circular annulenes, polyhexes, 2-dimensional graphene sheets and related structures including fullerenes, by focusing on spiroconjugated hydrocarbon structures in 1-, 2- and 3-D, including linear spiro[n]quinoids and polyspiroquinoid in 1-D, circular cyclospiro[n]quinoids, spiro[m,n]graphene fragments and spirographene in 2-D and [m,n,o]glitter fragments and glitter in 3-D.

1. Introduction

Recently the structure of the all-carbon "glitter" lattice [1] was described along with B_2C and CN_2 phases adopting this lattice. Glitter is a hypothetical

* Corresponding author.

tetragonal allotrope of carbon. The geometrical structure of the lattice (space group $P4_2/mmc$, # 131) is shown in figure 1.

The dimensions of the lattice are **a** = 2.53 Å and **c** = 5.98 Å, these are constrained by the geometry of the 1,4-cyclohexadiene molecule upon which the structure is based [2]. It is a 3-,4-connected net [3] containing trigonal and tetrahedral atoms in a ratio of 2:1, with a calculated density of 3.12 g/cm^3; intermediate between graphite and diamond. Apparent in the structure are the ethylenic columns which run perpendicular to each other to generate the 3-dimensional lattice.

Merz et al. [4] have described the electronic band structures of several related 3-,4-connected nets each possessing stacked olefin units. Evolution of

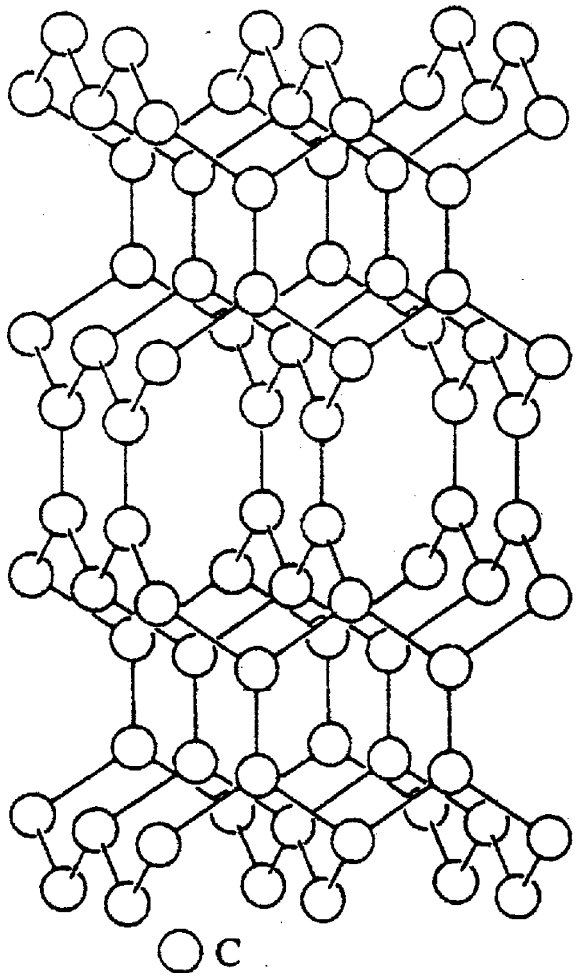

Figure 1. Structure of the glitter model in space group $P4_2/mmc$.

π–π* band overlap with the separation between adjacent units in an olefin stack is presented in their paper, this diagram is shown in figure 2. Note the touching of the π and the π* bands at an interaction distance of about 2.5 Å. From this diagram it is clear that the approximate density of states profile of glitter will be that of a metal, with a small π–π* band overlap at the Fermi level.

The structure shown in figure 1 also contains the 1,4-cyclohexadieneoid molecular units linked through their tetrahedral vertices to adjacent rings. These linkages form chains. Each such chain is termed a "polyspiroquinoid" substructure of the "glitter" lattice. The electronic structure of a polyspiroquinoid model is described below in connection with the concept of spiroconjugation.

Band structure calculations for this net were carried out using the extended Hueckel method adapted for application to extended structures [5]. Electronic band structures of various sublattice models, including the polyspiroquinoid one, were presented in the original report of the glitter structure [1] in order to clarify the importance of through-space interactions in these lattices.

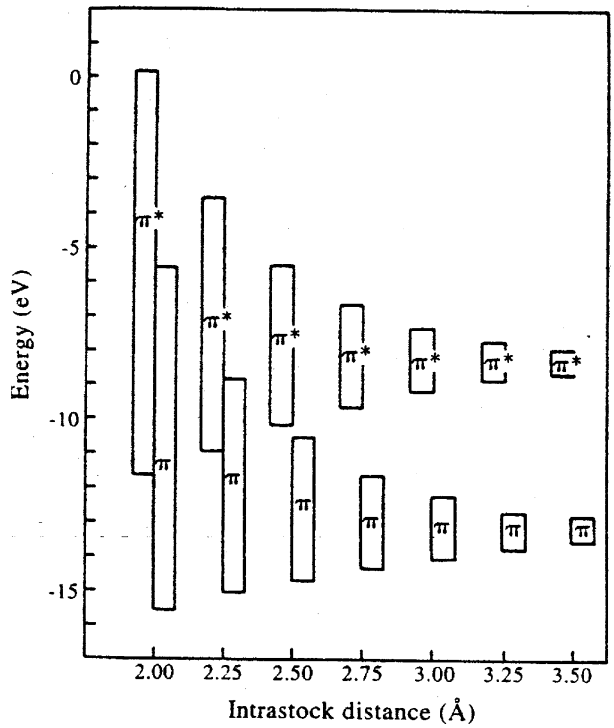

Figure 2. Evolution of π–π* overlap with the separation between adjacent units in an olefin stack.

2. Spiroconjugation in 1-dimension: polyspiroquinoid

Spiroconjugation [6] is claimed to occur in the electronic structure of the polyspiroquinoid chain [1]. This type of through-space interaction can be considered in terms of $4p_\pi$ atomic orbitals held "spiro" to each other about a tetrahedral C atom (see figure 3). These four orbitals interact to form four combinations of differeing symmetry with respect to the two perpendicular mirror planes dividing the tetrahedral C atom. One combination is symmetric under reflection in each mirror plane, labeled (SS), and there are also (SA), (AS) and (AA) combinations. The (AA) combination is shown, it is of the proper symmetry for a bonding spiro-type interaction.

From the original analyses of the effect of spiroconjugation in discrete molecular systems, including spiro[4.4]nonatetraene [7] the importance of it in stabilizing (and destabilizing) a frontier molecular orbital was of primary interest. This work was based upon electronic spectra, chemical reactivity and electronic structure calculations [6]. From this background, in the original paper on the glitter structure [1], only the lowest-lying π^* band, the LUCO (lowest unoccupied crystal orbital) was considered in assessing the importance of through-space p_{spiro} interactions in the 1-dimensional polyspiroquinoid substructure of glitter.

The interaction diagram for spiro[4.4]nonatetraene, reported by Duerr and Kober [7h], is shown in figure 4. The diagram reveals that in a situation involving $8p_\pi$ orbitals (four interacting π systems as opposed to four interacting p orbitals, as in figure 3), there are generated two sets of four butadieneoid π systems. These four butadieneoid π systems are of (AS), (AA), (AS) and (AA) symmetry, unlike the archetypal system diagrammed in figure 3. Interaction of these 4π systems through the spiro C atom, yields eight molecular orbitals over the skeleton of the spiro[4.4]nonatetraene molecule.

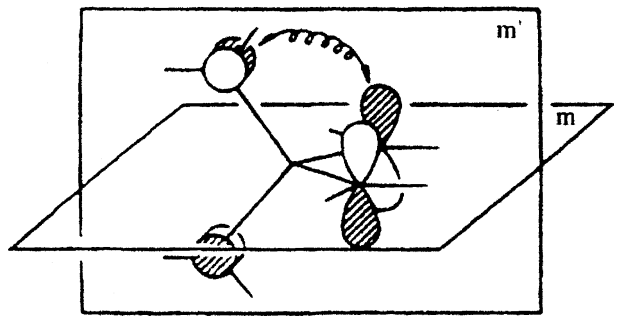

Figure 3. "Spiro" molecular orbitals derived from 4 p_{spiro} combinations. The (AA) combination is shown.

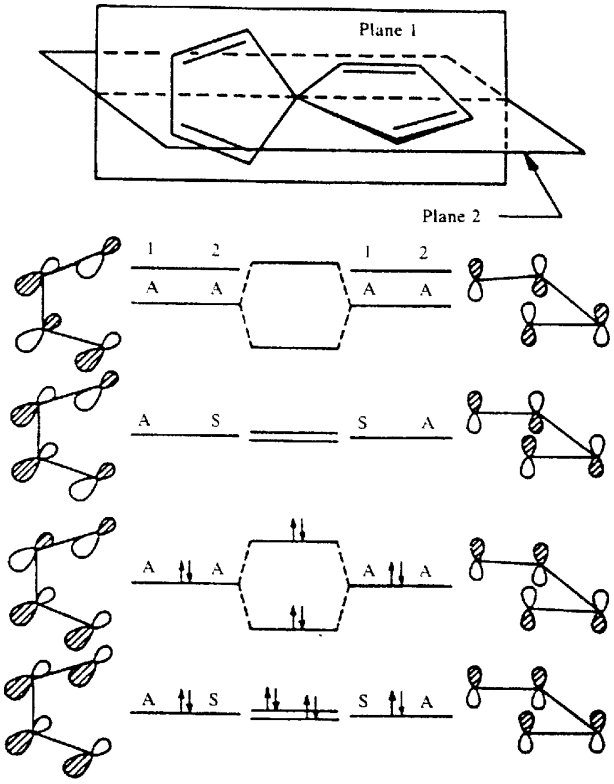

Figure 4. Molecular orbitals of spiro[4.4]nonatetraene.

Note the presence of the two (AA) combinations, one derived from the interaction of the HOMO (highest occupied molecular orbital) π levels of butadiene and one derived from the interaction of the LUMO+1 (next highest to the lowest unoccupied molecular orbital), π^* levels of butadiene. There are thus four levels in which the effects of spiroconjugation could be important, two down in the bonding manifold and the other pair in the anti-bonding manifold. The splitting of these pairs of (AA) combinations results from one spiro[4.4]nonatetraene orbital carrying a bonding p_{spiro} interaction and its sibling carrying an anti-bonding p_{spiro} interaction.

An analogy exists between the interaction diagram of the spiro[4.4]nonatetraene molecule and the unit cell of the polyspiroquinoid chain. Certain of the energy levels in both of these systems are comprised of $8p_\pi$ atomic orbitals present in each structure. This analogy will be followed in the discussion below which describes the stabilizing effects of spiroconjugation in the electronic band structure of polyspiroquinoid.

Figure 5 shows the structure of the model polyspiroquinoid chain (H atoms added to the glitter fragment to reach a realistic structure) and figure 6 is its

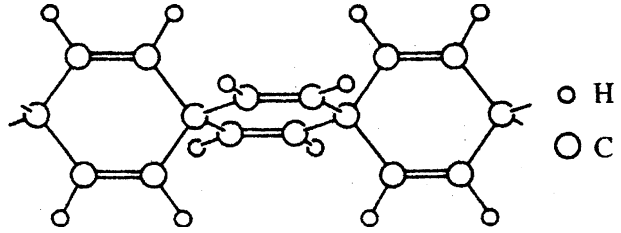

Figure 5. Structure of the polyspiroquinoid model.

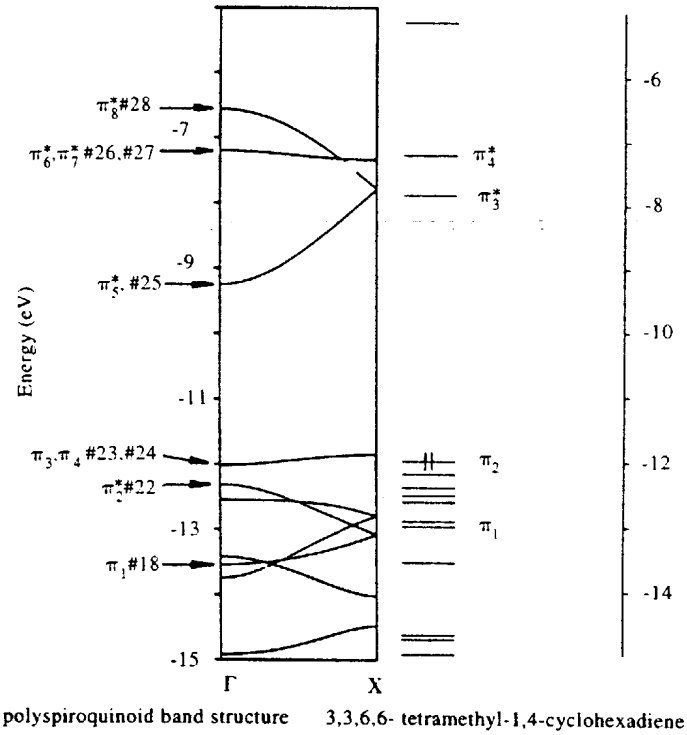

Figure 6. Electronic band structure of polyspiroquinoid and molecular orbitals of 3,3,6,6-tetramethyl-1,4-cyclohexadiene with π and π^* levels indicated.

electronic band structure. To the right in this diagram are appended the levels of the 3,3,6,6-tetramethyl-1,4-cyclohexadiene molecule. This molecule is a reasonable model for the polymer, but one lacking the spiroconjugation interaction. The 2π and $2\pi^*$ levels in the molecule have been indicated alongside the 4π and $4\pi^*$ bands of polyspiroquinoid.

As pointed out previously, [1] the lowest-lying π^* band in the electronic structure of the chain is of the proper symmetry (AA), for there to be a bonding p_{spiro} interaction in that band. In addition, the lowest-lying π band is also

of (AA) symmetry, so that there is a bonding p_{spiro} interaction in that occupied band as well. The relative importance of the effects of spiroconjugation in the chain will be posed with respect to the stabilization of the occupied π band compared to the energy level of the discrete π molecular orbital of 3,3,6,6-tetramethyl-1,4-cyclohexadiene from which it is derived.

In analogy with spiro[4.4]nonatetraene, the $8p_\pi$ atomic orbitals in the unit cell of polyspiroquinoid generate 4π crystal orbitals and $4\pi^*$ crystal orbitals in its electronic band structure. At the zone center, half of these eight crystal orbitals are constructed from real coefficients of the same magnitude at each p_π atomic site in the unit cell. Because of their importance in the analysis of spiroconjugation in polyspiroquinoid, these four (AA) crystal orbitals are sketched exactly as they occur at the zone center, in figure 7. These are analogous to the four (AA) combinations from the spiro[4.4]nonatetraene analysis. They occur as band #18 (π_1), band #22 (π_2), band #25 (π_5^*) and band #28 (π_8^*).

The four (AS) combinations occur in degenerate band pairs (compare to the orbital interaction diagram of spiro[4.4]nonatetraene) across the Brillouin zone of the chain. These are constructed from real coefficients of the same magnitude and sign at each p_π atomic site in one or the other ring of the polyspiroquinoid unit cell. Every other ring in the polymer possesses these π and π^* type interactions. The π and π^* interactions in half the unit cell are involved in σ or σ^* interactions with the adjacent ring, which maintain the (AS) symmetry of the crystal orbital. At the zone center they occur as bands #23 (π_3) and #24 (π_4) (the HOCO, highest occupied crystal orbital, levels) and as bands #26 (π_6^*) and #27 (π_7^*) (the LUCO+1 levels).

One can analyze the attendant orbital interactions of the (AA) combinations graphically from the sketches. In crystal orbital #18, the four bonding p_π

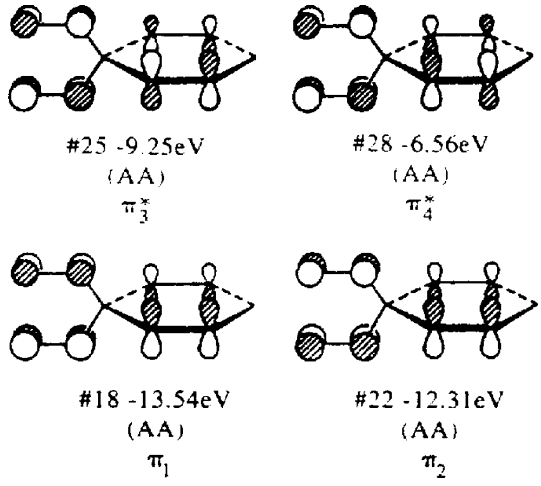

Figure 7. The p_π crystal orbitals of polyspiroquinoid sketched at the center of the Brillouin zone.

combinations in the unit cell also possess a bonding p_{spiro} interaction about each of the spiro carbons in the chain. Comparison with crystal orbital #22, the sibling π band to crystal orbital #18, reveals their only difference is the presence of an anti-bonding p_{spiro} interaction in the higher-lying π band. Their energy difference at the zone center is 1.23 eV, this is the actual magnitude of the splitting of the (AA) combinations; this was predicted qualitatively in the orbital interaction diagram shown in figure 4.

In the 3,3,6,6-tetramethyl-1,4-cyclohexadiene model molecule, the lower-lying π (π_1) level is the "out-of-phase" π combination, it is of (AA) symmetry with respect to the two mirror planes dividing the spiro carbon atoms in the ring. Its sibling level (π_2) is the "in-phase" π combination, it is of (AS) symmetry. The 2π (AA) levels in polyspiroquinoid are derived from the pure "out-of-phase" π combination of this model molecule, and the two (AS) levels are derived from the pure "in-phase" π combination. Crystal orbital #18 (π_1) occurs at -13.54 eV at the zone center and crystal orbital #22 (π_2) occurs at -12.31 eV. Therefore the spiroconjugation band is stabilized by 0.55 eV with respect to the lower-lying π level in 3,3,6,6-tetramethyl-1,4-cyclohexadiene and its sibling π band, with anti-bonding p_{spiro} interactions, is destabilized by 0.68 eV.

Tracing the evolution of these bands along the symmetry line of polyspiroquinoid, one sees the two sibling bands meet at the zone edge where they are degenerate (see figure 6). This degeneracy occurs because of the presence of a 4_2 screw axis in the polyspiroquinoid unit cell. The band structure is "folded" in half due to the 4_2 screw axis. Across the Brillouin zone crystal orbital π_1, the spiroconjugation band, is stabilized with respect to the lower-lying π level in 3,3,6,6-tetramethyl-1,4-cyclohexadiene (π_1). At the zone edge, the degeneracy at -13.07 eV is just 0.08 eV below the corresponding molecular orbital (π_1) in the 3,3,6,6-tetramethyl-1,4-cyclohexadiene model molecule.

Figure 8 shows the density of states (DOS) diagram along with the band structure diagram (figure 6) of polyspiroquinoid. The shaded area is the contribution of p_π orbitals to the total DOS. It has a "spike" at an energy which corresponds to the spiroconjugation band at the zone center (-13.5 eV). This spike indicates there is a large density of states in the electronic structure of the polymer at that energy. Evidently from the DOS diagram, there is not a corresponding spike coincident with the energy of the sibling π band which possesses anti-bonding p_{spiro} interactions at the zone center. This is consistent with the small degree of dispersion (flatness) of band #18 in the neighborhood of the zone edge.

3. Spiroconjugation in 3-dimensions: glitter

In the full 3-dimensional glitter lattice shown in figure 1, it is obvious the polyspiroquinoid chains are linked together along the [100] and [010] directions

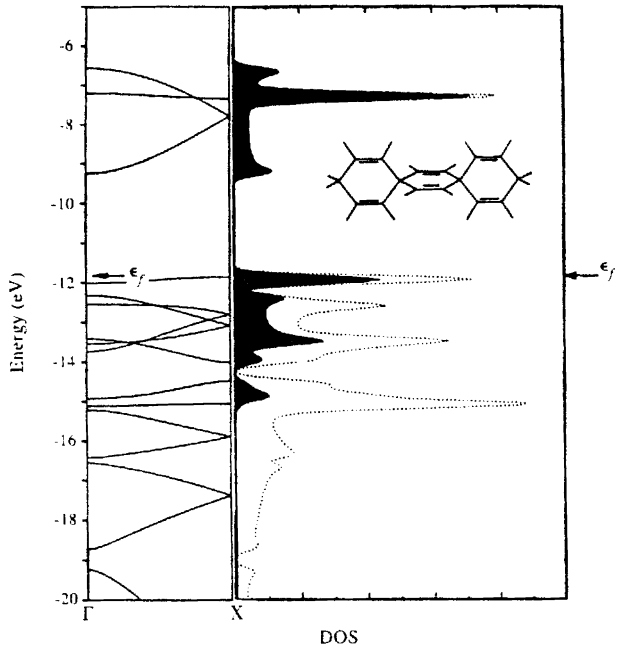

Figure 8. Electronic band structure and density of states (DOS) of the polyspiroquinoid model; shaded area indicates contribution of p_π orbitals to the total DOS.

of the lattice. Although through-space bonding p_σ interactions are primary in the analysis of what occurs at the Fermi level of glitter, it turns out that the spiroconjugation effects seen in the 1-dimensional polyspiroquinoid substructure will carry over into the 3-dimensional structure.

As is implied in the model structural drawing on the inset of figure 9, through-space bonding p_σ interactions are responsible for reducing the band gap (see figure 2) in the 1-dimensional polycyclophane substructure, which possesses the p_σ interactions uniquely among the 1-dimensional substructures. Clearly in this substructure, which from its geometry is absent orbital interactions connected with spiroconjugation, the π and π^* crystal orbitals come in pairs, the HOCO-1 and the HOCO as the π bands, and the LUCO and the LUCO+1 as the π^* bands. These bands run down from the zone center, where they occur in nearly degenerate pairs, out to the zone edge, as shown in figure 9.

Figure 10 shows the band structure of glitter, as there are six C atoms in the unit cell it consists of 24 bands, 12 of these bands are fully occupied. In order to assess the importance of through-space interactions in the lattice, including the importance of spiroconjugation, it is only necessary to consider the crystal orbitals derived from combinations of the p_π atomic orbitals present in the unit cell of glitter. These $4p_\pi$ atomic orbitals, one such atomic orbital for each of the four trigonal planar C atoms in the unit cell, combine together to form 2π crystal

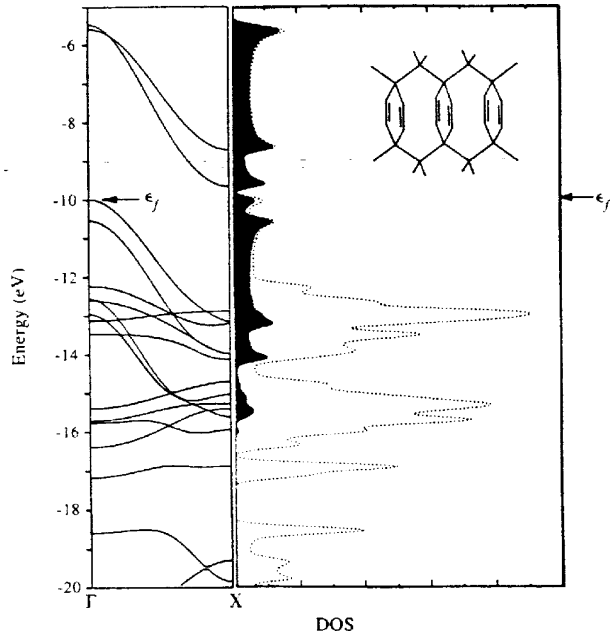

Figure 9. Electronic band structure and density of states (DOS) of the polycyclophane structure. Shaded area indicates the contribution of p_π orbitals to the total DOS. Structural model shown on onset.

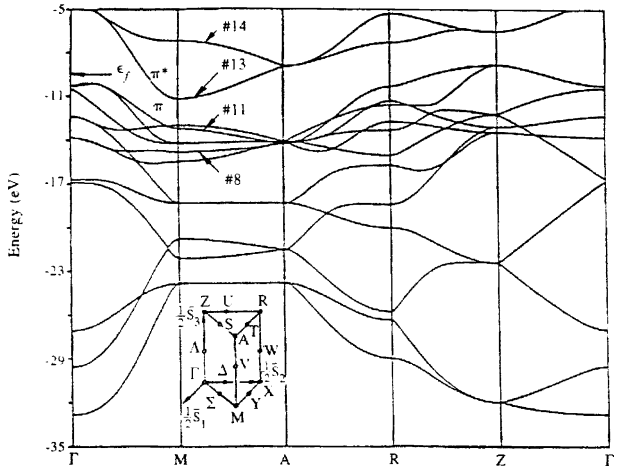

Figure 10. Electronic band structure of glitter. The π and π^* bands are indicated at symmetry point M of the Brillouin zone.

orbitals and $2\pi^*$ crystal orbitals in the electronic band structure of the glitter lattice.

In analogy with the polycyclophane substructure, it would be expected that these π and π^* crystal orbitals would bracket the Fermi energy; that is they would occur as the HOCO-1, HOCO, LUCO and LUCO+1 (see figure 10). In the original report of the electronic structure of glitter, the authors pointed to the importance of through-space p_σ interactions, occurring together with through-bond p_π interactions, at the short interaction distance of 2.53 Å present in the unit cell.

Comparison of the Brillouin zone of glitter to the unit cell of glitter in direct space, shown on the inset of figure 10, reveals that symmetry point M is analogous to the zone center in the Brillouin zone of the polyspiroquinoid model. The symmetry line from M to A corresponds to the symmetry line followed from the zone center to the zone edge in the electronic structure of the polyspiroquinoid model. The π and π^* bands in glitter, the π bands labeled as #8 and #11 and the π^* bands labeled as #13 and #14, at symmetry point M in the diagram, become degenerate pairs at symmetry point A. These degeneracies occur because of the presence of a 4_2 screw axis in the unit cell of glitter.

At symmetry point M in the Brillouin zone of glitter these four crystal orbitals enter with real valued coefficients of the same magnitude. It is possible to carry out a graphical examination of these four crystal orbitals derived from the 4 p_π atomic orbitals of glitter. They may be sketched exactly as they appear in the Brillouin zone at symmetry point M. From these sketches, which are shown in figure 11, the attendant orbital interactions may be analyzed graphically.

Labeling the 4π crystal orbitals at high symmetry point M in the Brillouin zone, using their symmetry with respect to the 4_2 screw axis and the **c** glide plane of the unit cell, there are four combinations: π_1 (SS), π_2 (AA), π_3^* (AA) and π_4^* (SS). Using the two mirror planes along [001] to assign the symmetries of the π crystal orbitals, instead of their behavior with respect to the space symmetry elements, they would all be of symmetry (SS), this represents an inversion of symmetry from the polyspiroquinoid (AA) combinations. Had the unit cell been chosen with [100] and [010] rotated through 45° from the present unit cell, all four combinations would be of (AA) symmetry with respect to the two mirror planes along [001]. This is entirely analogous to the four (AA) combinations of the polyspiroquinoid model, although not strictly homologous to the electronic structure of the polymer, as is discussed later. At any event, the present choice of unit cell makes visualization of the orbital interactions more clear to the reader.

From these sketches, one can see the presence of p_π interactions within the unit cell and also the presence of inter-cell and intra-cell p_σ and p_{spiro} interactions. Band #8 is the lowest-lying π crystal orbital (−14.87 eV), labeled π_1 (SS). It possesses through-space bonding p_{spiro} interactions and lies 1.67 eV below the next highest π crystal orbital, band #11 labeled π_2 (AA) (−13.25 eV) at symmetry point M. This splitting is analogous to the splitting of the bonding (AA)

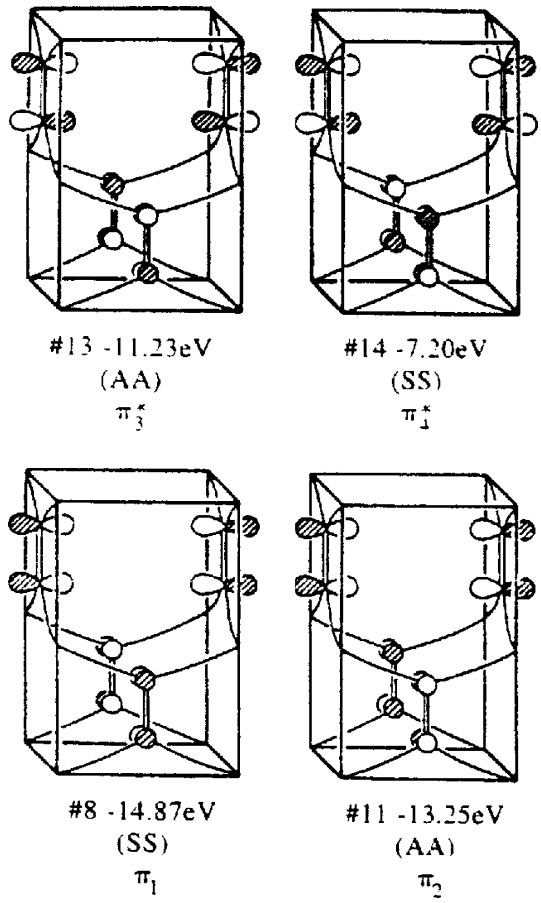

Figure 11. $40p_\pi$ crystal orbitals of glitter at symmetry point M in the Brillouin zone.

combinations in polyspiroquinoid. Bands #13 and #14 are the $2\pi^*$ crystal orbitals at M, they differ only in that the lower-lying of the pair has bonding p_{spiro} interactions, they have an energy separation of over 4 eV.

At this symmetry point in the Brillouin zone, the spiroconjugation effects present in the unit cell of glitter provide a stabilization energy of 1.93 eV compared to the energy of the "out-of-phase" π combination (π_1) of 3,3,6,6-tetramethyl-1,4-cyclohexadiene (see figure 6). The destabilized sibling π band (AA), at -13.25 eV, is itself 0.26 eV stabilized with respect to the "out-of-phase" π combination of the 3,3,6,6-tetramethyl-1,4-cyclohexadiene model molecule. Evidently, the p_σ interactions are quite important in stabilizing this π_2 (AA) crystal orbital as well.

An indirect band crossing of the lower-lying π^* band, the LUCO, with the HOCO and two other bands, is present in the band structure of glitter (see fig-

ure 10). Of the $2\pi^*$ crystal orbitals present in the electronic structure of glitter, the π^* crystal orbital which is the LUCO has through-space bonding p_{spiro} interactions (along with the p_σ interactions) which cause this band to dip to a minimum that crosses indirectly the lower-lying occupied bands in glitter. This is pictured in figure 11 and thus explains the origin of the synthetic metallic status adopted by this hypothetical allotrope of C.

Figure 12 shows the electronic band structure for the glitter lattice in the energy window from -15 to -5 eV. Inspection of this calculated band diagram shows that the lowest-lying π band, band #8, occurs at its lowest energy point at symmetry point M in the Brillouin zone, as does the lower-lying π^* crystal orbital. The lowest-lying π band is the HOCO-4, not the expected HOCO-1.

It occurs as such through the entire Brillouin zone of glitter. Band #11, refer to the corresponding sketch in figure 10, is the next highest π band, it forms a degenerate pair as the highest occupied crystal orbital along the symmetry line from Z to Γ in the Brillouin zone of glitter. Inspection of the Brillouin zone (figure 12) reveals that the 2π crystal orbitals maintain an energy separation of about 1 eV throughout most of the reciprocal space of glitter.

Note also in figure 12, the small dispersion (flatness) of band #8 about symmetry point M in the Brillouin zone, this gives rise to the secondary peak in the DOS of glitter (see figure 13), at an energy of about -15.0 eV. The shaded area indicates the contribution of p_π orbitals to the total DOS. The primary peak occurring at about -13.0 eV nearly coincides with the flatness of the sibling π crystal orbital, band #11, about this symmetry point in the Brillouin zone of glitter.

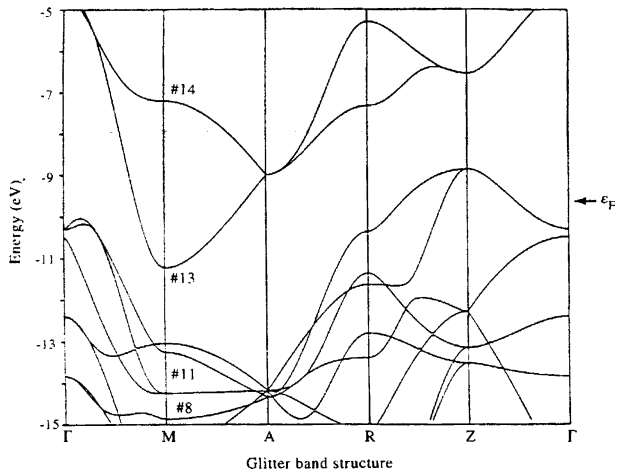

Figure 12. Electronic band structure of glitter in the energy window from -15 to -5 eV.

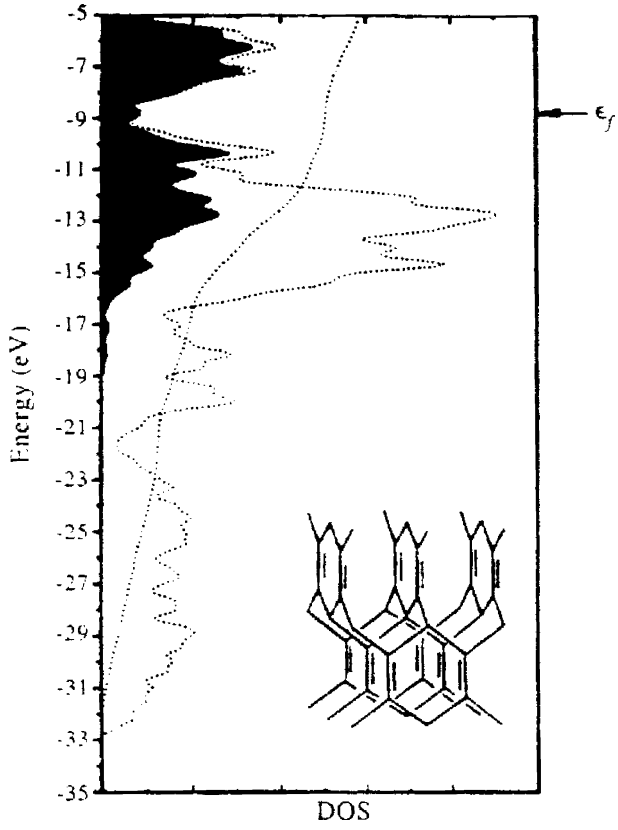

Figure 13. Density of states (DOS) of glitter. Shaded area indicates the contribution of p_π orbitals to the total density of states.

4. The special crystal orbital of glitter

Inspection of the atomic orbital composition of band #8 of glitter, the lowest-lying π crystal orbital, at symmetry point M in the Brillouin zone, reveals it has all 4 p_π coefficients entering with the *same magnitude and sign*. Because of the presence of a bonding p_π interaction, two bonding p_σ interactions and four bonding p_{spiro} interactions about e*very* p_π atomic orbital in the unit cell of glitter, this is termed its special crystal orbital. This is diagrammed in figure 14. The effects of spiroconjugation along with the other interactions present in this 3-,4-connected network may confer it with an unusual electronic stability akin to the aromaticity observed in the planar polyhexes and 2-D graphene sheet of ordinary quantum chemistry[8].

The special crystal orbital can be viewed in sections through several unit cells perpendicular to the (001) plane of the tetragonal structure, and with the spiro atoms flattened out for clarity, as is shown in figure 15 (this diagram is

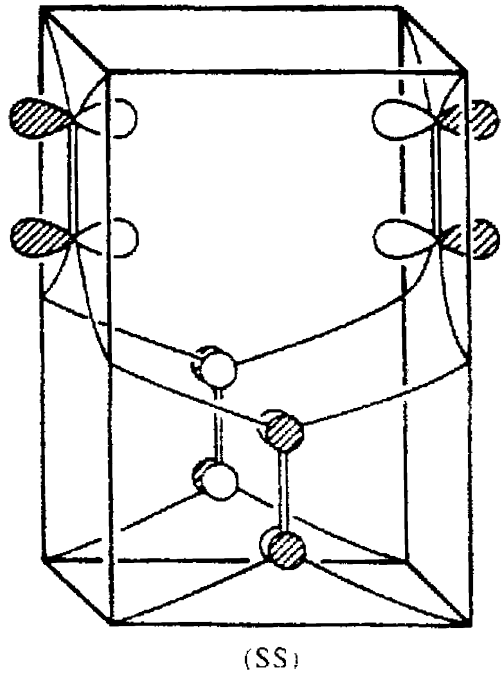

Figure 14. The special crystal orbital of glitter.

applicable to the view of the lower-lying π^* crystal orbital, the LUCO, perpendicular to (001) as well, however alternating sheets would be out of phase along the 3rd dimension in the LUCO). Note the resemblance of this pattern to that of a standard checkerboard square, it arises as a consequence of the tetragonal symmetry of the glitter structure and from the nature of the p orbital interactions admitted by the glitter lattice. The constructive interactions present in the unit cell involve intra-cell interactions: p_π, p_σ and p_{spiro}; and inter-cell interactions of the same nature.

5. Exo- and endo-spiroconjugation and diffraction

Self assembly involving four allene units per reaction, in the presence of a catalytic amount of the organometallic reagent bis-(triphenylphosphite)-nickeldicarbonyl, has been reported to produce 1,3,5,7-tetramethylenecyclooctane [10]. Synthesis of 1,3,5,7-tetramethylenecyclooctane represents the 1st example of a molecular system with the possibility of exhibiting the effect of endo-spiroconjugation. Well known in structural chemistry are the homologies provided by the hydrocarbon molecules naphthalene and adamantane, which have very nearly the carbon–carbon bond lengths and bond angles, respectively, of their homologous extended structures: graphite and diamond [9]. From

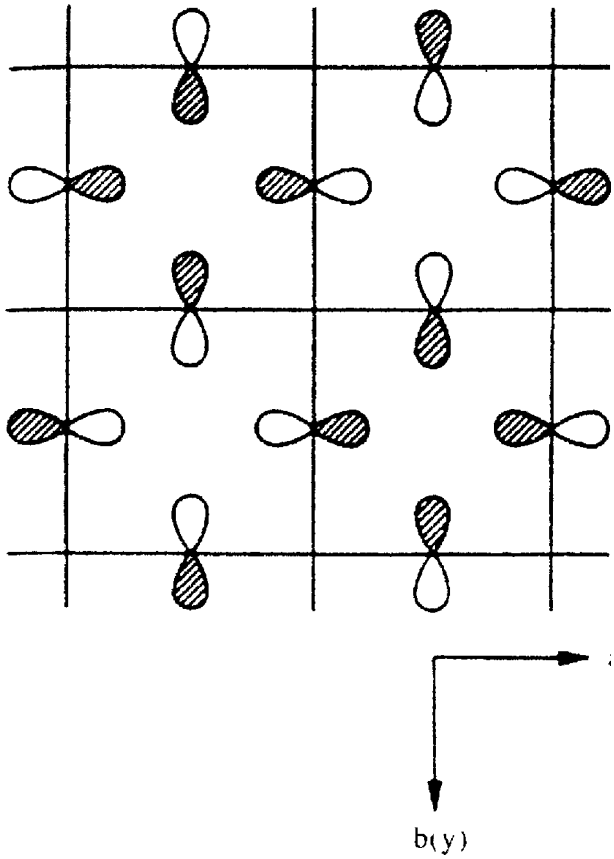

Figure 15. "Sections" of the special crystal orbital along [100] and [010] lattice directions. View is perpendicular to (001).

this perspective, the synthesis of 1,3,5,7-tetramethylenecyclooctane provides the opportunity to have an homologous hydrocarbon fragment of the structure of glitter which can be studied experimentally.

Endo-spiroconjugation, potentially present in the 1,3,5,7-tetramethylenecyclooctane molecule, is precisely the mechanism of spiroconjugation that would occur intracellularly and extracellularly in the glitter lattice, please refer to the previous sections for details. Literature previously cited on aspects of spiroconjugation [7] concerned the related effect of exo-spiroconjugation, the interaction diagram of which is shown in figure 3 (interaction of 4p orbitals) and figure 4 (interaction of 4π orbitals). As discussed in the section 2, in the hypothetical polyspiroquinoid polymer, exo-spiroconjugation is operative.

Ideally, endo-spiroconjugation involves 4p orbitals that point along lines, through space, which represent a pair of *edges* of a perfect tetrahedron, held at right angles to each other. Oppositely, exo-spiroconjugation, as pictured in

figure 3, involves 4p orbitals which are centered at each *vertex* of a tetrahedron and point at right angles, in two different pairs, respectively, each to one of a corresponding pair of orthogonal tetrahedral edges. Thus, the tetrahedron in exo-spiroconjugation is formed from $4sp^3$ hybrid orbitals extending from the spiro C atom to each of the atoms possessing the interacting p orbital. Quite in contrast, the p orbitals at a site of endo-spiroconjugation are cenetered on a point in space. From this subtle difference it is apparent that, site-by-site, the p orbital endo-spiroconjugated sees each of the $2p_{spiro}$ interactions of its counterpart p orbital that is exo-spiroconjugated; *and simultaneously it sees a* p_σ *interaction*.

In the structure of 1,3,5,7-tetramethylenecyclooctane, ideally the effect of endo-spiroconjugation should manifest itself in the geometry of the skeletal cyclooctane ring system; the four trigonal atoms in the ring should inscribe a perfect tetrahedron inside the octagonal cradle. At the center of the inscribed tetrahedron, a significant π electron density should be present from the four-center interaction of endo-spiroconjugation. As the scattering power for X-rays depends upon the electron density, diffraction patterns obtained from molecular crystals of the 1,3,5,7-tetramethylenecyclooctane molecules may indicate weak reflections corresponding to the electron density $\rho_{spiro}(x, y, z)$ at the fractional coordinates of the unit cell specifying the center of the inscribed tetrahedron in the cyclooctane cradle (the center of symmetry of the molecule). Alternatively, electron density maps of the structure of 1,3,5,7-tetramethylenecyclooctane calculated by direct methods from the original diffraction data would reveal, quantitatively, the magnitude of π electron density at the fractional coordinates corresponding to the center of symmetry of the 1,3,5,7-tetramethylenecyclooctane molecule.

Reflections due to π electron density concentrated at the center of symmetry of the 1,3,5,7-tetramethylenecyclooctane molecule would be weak for two principal reasons; the scattering power of the skeletal C atoms would be approximately 6 at low values of Θ; six being the number of electrons in C, whereas $\rho_{spiro}(x, y, z)$ could be at most approximately 2 at low values of Θ. The value 2 at low Θ is thus identified with the electronically unstable case that the π electron pair is cradled at the center of the inscribed tetrahedron. Intensity from $\rho_{spiro}(x, y, z)$ would be diminished substantially as the inscribed tetrahedron distorted from local T_d symmetry. As the non-ring C's in 1,3,5,7-tetramethylenecyclooctane are not stabilized by the benefit of endo-spiroconjugation, it is to be expected that the molecule will distort; it will maintain its principal S_4 axis, although it will distort towards a flattening out of the cyclooctane skeleton. Consequently, the local T_d symmetry of the inscribed tetrahedron will be lowered to one of D_{2d} symmetry and the scattering power at the endo-spiro center, $\rho_{spiro}(x, y, z)$, will be greatly diminished.

Construction of the model of the glitter lattice appealed to the geometry of the 1,4-cyclohexadiene molecule, information provided from diffraction studies [2].The carbon–carbon double bonds of the molecule are not conjugated and this

appears in the bond alternation, the carbon–carbon single bonds being 1.51 Å and the carbon–carbon double bonds being 1.35 Å (in naphthalene the carbon–carbon bond lengths are approximately 1.40 Å, and in adamantane the carbon–carbon bond lengths are approximately 1.54 Å, respectively). Similarly, the bond angles are unsymmetrical in 1,4-cyclohexadiene with the C=C−C angles being 123° (ideal trigonal angle is 120°) and the adumbrated C−C−C angles are 114° (ideal tetrahedral angle is 109°28′).

Bond length and bond angle alternation present in the 1,4-cyclohexadiene molecule, and consequently the glitter lattice which is based upon it, distinguishes glitter from the metrically ideally regular sibling structures: graphite and diamond. See a later section for a further description of this metrical difference. Also discussed later, the standard topological indexes, polygonality and connectivity, distinguish glitter further as a topologically irregular (i.e., Wellsean) structure, while two of its siblings, graphite and diamond, are regular 2-dimensional and 3-dimensional structures, respectively; and the 3rd group of its siblings, the crystalline fullerenes, are semi-regular polyhedra (i.e., Archimedean).

Apparently quite by accident, the irregular metrical properties of the glitter lattice; the bond angle and bond length alternation, concomitant with its "low" topology (see a later section), result in the occurrence of nearly perfect tetrahedra, centered in space, which are about 2.5 Å on an edge. Such tetrahedra, being centered in space as opposed to being centered at an ideally tetrahedral C atom, as in diamond for example, provide the vehicle within which the four center p orbital interaction of endo-spiroconjugation may occur. These tetrahedra possess nearly the full T_d symmetry that is evidently required for the optimum energetic stabilization associated with endo-spiroconjugation, refer to the earlier sections for a quantitative measure of this interaction energy.

Superimposed upon the unit cell of glitter; interpenetrating with it, which itself is outlined by the positions occupied by the 6 C atoms in $P4_2/mmc$ in glitter, are the set of points coincident with the spatial centers of the nearly perfect tetrahedra. These are the sites at which, through the effects of endo-spiroconjugation, are concentrated the π electron density from the four center, through-space interaction. The latter array constitutes a primitive tetragonal lattice of points (P4/mmm) which is half the volume of the unit cell of glitter, the secondary lattice having its origin centered at (1/2,1/2,0) of the primary glitter lattice. Each of these sites may have a scattering power approaching two at low X-ray scattering angles, Θ. In light of the T_d symmetry of these sites, and the more closely-spaced, regular array of such sites in the glitter lattice, compared to the situation in a molecular crystal of 1,3,5,7-tetramethylenecyclooctane discussed previously, it is to be expected that any weak reflections associated with X-ray scattering from the sites of $\rho_{spiro}(x, y, z)$ in glitter would be more evident than in a comparable diffraction pattern of a molecular crystal of 1,3,5,7-tetramethylenecyclooctane.

6. Exo- and endo-spiroconjugation and chemistry

Williams and Benson [10] report aspects of the chemistry of 1,3,5,7-tetramethylenecyclooctane which provides some evidence for the proximity of π electrons within the cradle of the cyclooctane ring system. Effects on chemical reactivity due to exo-spiroconjugation have been referred to earlier [7]. It was hoped that evidence for the proximal interaction of adjacent, exocyclic methylene groups of the molecule would be evident through the formation of a transannular bond, in analogy with the cycloaddition reaction of tetracyanoethylene with bicycloheptadiene producing nortricyclene [11]. Cycloaddition of tetracyanoethylene with 1,3,5,7-tetramethylenecyclooctane falls within the class of symmetry-allowed, thermal s,s,s reactions; it is a $[_{\pi}2_{s} +_{\pi}2_{s} + {}_{\pi}2_{s}]$ cycloaddition reaction [12].

Tetracyanoethylene was chosen as the reagent to establish the interaction of pairs of opposite double bonds, the ring carbon p orbitals of which point towards each other along a line corresponding to one of the two orthogonal edges of the tetrahedron inscribed in the cradle of the cyclooctane skeleton, described above. An approximately equimolar reaction mixture of the two was prepared in tetrahydrofuran (THF) at room temperature. An exothermic reaction occurred within minutes, and after an hour the product was isolated, crystallized from acetonitrile and from spectroscopis analysis was determined to have a 3,3,4,4-tetracyano-8,11-dimethylenetricyclo[4.3.3.0]-dodecane structure. As the author's pointed out, "this appears to be the first example in which transannular bond formation can be directly attributed to the *proximity* of exocyclic methylene groups" [10].

7. Distortions of the glitter lattice

Based upon the crystal structures of diamond and graphite [9], in which the bond lengths and bond angles are uniform within each structure, respectively, a distortion was performed on the glitter lattice such that the bond lengths were all fixed at 1.46 Å (instead of alternating between 1.35 and 1.51 Å) and the bond angles were all fixed at 120° (except around the circumference of the tetrahedral C atoms, which is constrained to about 105°). The distortion to a more metrically regular structure destabilized the lattice by 0.80 eV/C atom relative to the metrically irregular structure.

Evidently, as the metrical properties of the lattice are modified to be more uniform, the tetrahedral sites that are centered in space, associated with the four center p orbital interaction of endo-spiroconjugation, concomitantly undergo a lowering of their local symmetry from T_d to D_{2d}. This is consistent with the model of endo-spiroconjugation presented here, in which the ideality of the tetrahedron yields optimum stabilization from the effect of endo-spiroconjugation.

8. Synthesis of glitter

Glitter is a 3-,4-connected net, so it is to be expected that a synthesis would be possible at conditions of temperature (T) and pressure (P) dictated by the phase boundary between graphite and diamond. However, the recent literature on C reflects the importance of kinetically driven syntheses, especially at conditions of T and P other than those along the graphite-diamond phase boundary. These include syntheses with vaporous carbon and hydrocarbon precursors in deposition apparatus [13]. A thermodynamic synthesis, in the vein of the original synthesis of diamond from graphite, could possibly be achieved in the presence of a suitable catalyst, such as a metallic solvent. Conventional high T-high P apparatus could be used for such a synthesis [14].

Identification of phases produced in such synthetic programs would principally include the use of diffractometry and spectroscopy. From the details of the electronic band structure of glitter reported herein, it should be possible to assign π–π^* electronic transitions through the analysis of the UV-visible absorption spectra, photelectron spectroscopy should elucidate features of the highest occupied crystal orbital [15]. With regard to diffraction evidence, theoretical diffraction patterns could be calculated for various versions of the crystal structure of glitter and these theoretical diffraction lines could be searched for in a synthesis experiment such as one employing a diamond anvil synthesis cell (DAC) and synchrotron radiation.

9. Topological indexes of carbon allotropes and glitter

Wells' seminal work on the structures of 2- and 3-dimensional nets and polyhedra was organized through the use of topological labels called Schlaefli symbols [3]. In such a scheme, there are two indexes, the polygonality represented by n and the connectivity represented by p. Each polyhedron, plane tessellation and 3-dimensional net has a Schlaefli symbol (n, p) to label its location in the space of topological structures in which Wells worked [16]. Interestingly, the Schlaefli symbols are rigorously determined for the convex polyhedra through a relation due to Euler.

Euler's work on the convex polyhedra resulted in an equation marking the origin of the discipline of topology, shown in one form as equation 1 [17].

$$V - E + F = 2. \tag{1}$$

Here V, E and F are the number of vertices, edges and faces, respectively, in the convex polyhedron [18]. Geometrical arguments can be used to transform equation 1 into forms relating V, E and F; the primary topological indexes, to n,

the polygonality and p, the connectivity; the latter being secondary topological indexes.

Each edge in a convex polyhedron is shared by two faces, therefore nF is the same as $2E$. Each edge has two vertices, therefore pV is the same as $2E$. By substitution, Euler's equation now reads:

$$\frac{2E}{n} - E + \frac{2E}{p} = 2. \tag{2}$$

Rearrangement of equation 2 into equation 3 shows that the values n, p and E must be positive integers for the expression to have validity for polyhedra [15]:

$$\frac{1}{n} - \frac{1}{2} + \frac{1}{p} = \frac{1}{E}. \tag{3}$$

Further restrictions are imposed on the values of n and p in order to determine the solutions to equation 3. In order for the number of edges, E, to be positive the values of n and p must be less than 6, and in fact n and p must be greater than 2 because of the impossibility of faces of zero area or spikes in the convex polyhedron.

Substituting each of the nine combinations of 3–5 into equation 3, there are only five finite, rational solutions. The five are well known and are shown as the tetrahedron, t, the octahedron, o, the icosahedron, i, the cube, c, and the dodecahedron, d, in the table 1.

Of the other four non-solutions, from the square net (4, 4) substitution into equation 3 indicates the number of edges, E, in this structure is infinite. Evidently, in (4, 4) the Euler equation reveals a transition to a 2-dimensional extended structure [19]. In (4, 5), (5, 4) and (5, 5) the non-solutions have values of -5, -5, and -10, respectively. Another transition has occurred, to a still higher dimensionality, specifically to 3-dimensional structures. (5, 5) corresponds to a 3-dimensional network that Wells first discovered in the 1960s [3]. For a

Table 1
Schlaefli symbols for regular structures.

	P					
n	3	4	5	6	7	8
3	t	o	i	(3,6)	(3,7)	(3,8)
4	c	(4,4)	(4,5)	(4,6)	(4,7)	(4,8)
5	d	(5,4)	(5,5)	(5,6)	(5,7)	(5,8)
6	(6,3)	(6,4)	(6,5)	(6,6)	(6,7)	(6,8)
7	(7,3)	(7,4)	(7,5)	(7,6)	(7,7)	(7,8)
8	(8,3)	(8,4)	(8,5)	(8,6)	(8,7)	(8,8)

sensible result, in which the number of edges, E, is positive, it is clear that a modification of the classical Euler equation, one applicable for 3-dimensional networks, is necessary [20].

The structure of the graphite net is well known, its Schlaefli symbol is (6, 3), the polygonality is 6 and the connectivity is 3. Its place in the topological subspace comprised of regular structures, regular meaning the Schlaefli symbols n and p are integers, is to the right of the convex polyhedron (5, 3), which is the pentagonal dodecahedron, and to the left of (7, 3). Interestingly, (7, 3) represents a group of at least four unique, regular nets which Wells discovered [3]. To date, none of these nets in the family (7, 3) has yet been discovered to correspond to an actual crystal structure.

Regular structures are adjoined to their left or right, or adjacent to them vertically, by the semi-regular structures, semi-regular meaning that one of the Schlaefli indexes n and p is fractional and the other is an integer. One such semi-regular with contemporary importance is the Archimedean polyhedron called the truncated icosahedron. The Schlaefli symbol for this mathematical object, and for the Buckminsterfullerene molecule that is patterned after it, is given by $(5^{2/3}, 3)$. It is intermediate in topology between the pentagonal dodecahedron (5, 3) and the graphite net (6, 3). Buckminsterfullerene is unique among the allotropes of C in that it is semi-regular.

Classical structures include the regular and Archimedean polyhedra; Archimedean meaning only n, the polygonality, is fractional. In the 19th century, Catalan identified the reciprocal polyhedra to the Archimedean polyhedra where n and p were exchanged with each other. Catalan polyhedra can be constructed from their reciprocals by joining the midpoints of each face of the Archimedean polyhedron to each other [21]. This reciprocal nature occurs also in 2-dimensions, one can easily visualize the reciprocals of (4, 4), (3, 6) and (6, 3) for example; but is apparently absent in 3-dimensional nets.

Beyond the semi-regular structures lie the Wellsean structures, those in which both the polygonality n and the connectivity p are fractional, in the Schlaefli symbol (n, p) [22]. These structures would lie diagonally, to the left or right and displaced vertically, from the entries into the table of Schlaefli symbols for the regular polyhedra, plane nets and 3-dimensional nets. Wells discovered many Wellsean structures, specifically classifying them as possessing fractional polygonality and fractional connectivity, in the course of his exploration of the space of 3-,4-connected nets [22].

It appears that the first actual Wellsean structure was identified, though not topologically indexed as such, by Bragg and Zachariasen, from their determination of the crystal structure of the silicate mineral called phenacite, Be_2SiO_4 [23]. This was an especially difficult structure determination because of the rhombohedral symmetry (R3) and the large size of the unit cell (six molecules of Be_2SiO_4 in each unit cell). In Bragg's description he reports, "It is difficult to give a clear figure of the structure, because the unit cell is large and a

pattern with rhombohedral symmetry is harder to depict than one based upon rectangular axes. The principles of the structure are very simple, however, and are readily traced in a model. It is formed of linked tetrahedra, with Si and Be at their centers. Each O of the independent SiO_4 groups also forms part of two neighboring tetrahedra around Be atoms. Thus each Si is surrounded by 4O atoms, and each Be by 4O atoms, and each O is linked to 2Be atoms and one Si atom at the corners of an equilateral triangle" [24].

With the identification of this structure type, which Bragg pointed out could be simplified by replacing the Be and Si atoms by one atom type, to a binary compound of formula A_3B_4 with a smaller unit cell with hexagonal symmetry ($P6_3/m$), entry had been made into a topologically new class of crystal structures. In such a hexagonal lattice, there are four 3-connected vertices and three 4-connected vertices in the asymmetric unit of structure, and there are six 6-sided polygons and four 8-sided polygons in the asymmetric unit of structure [9]. The Schlaefli symbol for the phenacite structure is therefore ($6^{4/5}$, 3.4285...). In 1939 and 1940, Juza and Hahn [2] synthesized and reported the crystal structure of Ge_3N_4, patterned on the structure of phenacite in the manner described by Bragg [26,27]. About 17 years later, the synthesis and crystal structure of another polymorph of Ge_3N_4, with nearly an identical density, and the corresponding syntheses of the isomorphous α- and β-Si_3N_4 polymorphs was reported in part by several groups including Hardie and Jack [26] and Ruddleson and Popper [27].

Motivated by the reports of the synthesis of the IV–V nitrides, 1st principles calculations were performed on a hypothetical carbon nitride phase, C_3N_4, patterned on the β-Si_3N_4 structure type [28]. A semi-empirical formula for bulk modulus developed out of this work, predicted the latter nitride would be of a hardness comparable to diamond [28]. Inspection of the glitter structure, a 3-,4-connected net with 6- and 8-sided polygons in its structural pattern, indicates the Schlaefli symbol (7, $3^{1/3}$). The polygonality is an admixture of 6's and 8's which nonetheless has the integer polygonality 7. It is a Wellsean structure. Its polygonality is higher that in the diamond structures (6, 4), and the graphene tessellation (6, 3), and the molecule Buckminsterfullerene ($5^{2/3}$, 3).

In a separate vein, Waser and McClanahan reported [29] the 1st transition metal-containing crystal structure of a 3-, 4-connected net, the Pt_3O_4 structure type, in 1951. As it turns out, this is a semi-regular structure (a Catalan network) with the Schlaefli symbol (8, 3.4285...). Here, as in the structures patterned on phenacite, the connectivity appears as a continued fraction. It might be expected that the symmetry of the structure would be low, on the basis of the low topology. Despite the irrationality of the connectivity, the Pt_3O_4 lattice possesses cubic space group symmetry (Pm3n). The IV–V nitrides are of hexagonal symmetry ($P6_3/m$). Topology (regularity) and symmetry are to some degree independent properties of structures. Even so, the well-known structures of graphite and diamond, for example, independent of their high symmetry, possess high topology.

In 1965, Wells [3] reported two new semi-regular (Catalan) 3-,4-connected nets; 2 unique nets possessing the same Schlaefli symbol (8, 3.5714...). Their topological identity is not distinguishable completely by their Schlaefli symbol, as in other cases, and a distinct topological identity is provided through the use of further labels based upon the number of polygons common to each link and vertex, respectively. In fact one net is comprised of square planar connectivity (space group I4/mmm) and the other contains tetrahedral connectivity (space group I4m2). Both of these nets possessed trigonal planar vertices bonded with 4-connected vertices. Moreover, a 3rd 3-,4-connected net was reported in this paper, this net with the Schlaefli symbol ($8^{1/2}$, $3^{1/3}$). It possesses orthorhombic symmetry (Pmmm). With this work, Wells began his exploration of the 3-,4-connected networks and began identifying Wellsean networks.

Physically, the polygonality is approximately related to the openness of the structure. The connectivity index is approximately related to the closedness of the structure. For example, the glitter structure has a connectivity index of $3^{1/3}$, it is clearly intermediate between graphite at 3, and diamond at 4. From the connectivity index it can be identified topologically as a hybrid of graphite and diamond. Compare to the Buckminsterfullerene molecule, with a polygonality of $5^{2/3}$, it being intermediate between the pentagonal dodecahedron (5, 3) and the graphene tessellation (6, 3). Another useful topological index obtained from the polygonality and the connectivity, is formed by taking the ratio of n and p:

$$l = \frac{n}{p}, \tag{4}$$

where l is a measure of the form of the structure as related to its average polygon size per unit average connectivity. It is a topological index useful in one sense for identifying similarities between regular, semi-regular and Wellsean structures.

Along the principal diagonal of table 1 are structures in which the polygonality is the same as the connectivity, the topological index l is therefore unity. Such structures have the very highest topology. To the left of the principal diagonal lies the subspace of structures with l indexes less than one, to the right of the principal diagonal lie structures with indexes l greater than one. As a general index of topological relatedness, it is very interesting to note graphite and glitter both possess l indexes close to 2. It is hoped that this indicial similarity can be elucidated in a future communication about graphite and glitter.

Consideration of the work on 3-, 4-connected nets initiated with Bragg and Zacharaisen in 1930 on phenacite; followed by Juza and Hahn in 1940 and Ruddleson and Popper, and Jack and Hardie in 1957, on IV–V nitrides; then the theoretical work of Wells on the 3-, 4-connected networks begun in 1965; and most recently the attempts by the group led by Cohen to synthesize C_3N_4 in the 1990's; there is a clear progression towards the synthesis of 3-,4-connected nets of the 2nd period elements. Quite apart from this development, though

apparently converging with it, is the descendency of synthetic allotropes of C from those C nets possessing a high topology, to new forms of C which break to lower topologies, the principal example of which is the self assembly of the Buckminsterfullerene molecule [13].

Isomorphous variants of the parent lattice of C atoms, are the III–IV series of compounds which could adopt the glitter structure. The fully metallic band profile of the hypothetical B_2C phase patterned on the glitter structure, has been briefly described [1]. Alternatively, the adjacency of trigonal centers across faces in the unit cell of glitter, suggests a denser structure in which trigonal planar points are transformed into trigonal bipyramidal points. Such a lattice would appear to be the first 4-, 5-connected net, and a good model for exploration of 3rd period IV–V structures which have access to expanded octet hybridization (sp^3d) about the group V elements, for example phases such as SiP_2.

10. The foundations of a spiro quantum chemistry

With the foregoing analysis of spiroconjugation presented with respect to the 1-dimensional polyspiroquinoid polymer and the 3-dimensional glitter structure, the foundations have been laid for the elucidation of a new type of quantum chemistry, called spiro quantum chemistry. Spiro quantum chemistry complements the historically developed quantum chemistry of linear polyenes, the annulenes, polyhexes, 2-D graphene sheets and the fullerenes. Fragments of the polyspiroquinoid polymer, called the spiro[n]quinoids, constitute the spiro quantum chemistry analogs to the linear polyenes. If one joins the spiro[n]quinoids at their ends, one forms the cyclospiro[n]quinoids. Thus the cyclospiro[n]quinoids constitute the spiro quantum chemistry analog to the annulenes of ordinary quantum chemistry. As they possess analogous nodal properties, in the spiro wave functions, to the ordinary π and π^* wave functions of the linear polyenes and the cyclic annulenes, it may be possible to identify an analog of the "$4n + 2$" rule of aromaticity in the cyclospiro[n]quinoids.

In 2-dimensions one has the analog of the graphene sheet reported as the spirographene sheet in [1]. It's band structure shows it to be semi-metallic, in analogy with the ordinary graphene sheet. Fragments of the graphene sheet are termed poly[m,n]hexes, where the indexes m and n indicate the length and width of the polyhex fragment. In analogy to the poly[m,n]hexes there are the spiro[m,n]hexes, where the indexes m and n indicate the numbers of spiro nodes running lengthwise and widthwise in the spiro[m,n]hex fragment. From the band structure of the parent spirographene sheet, it is apparent that the spiro[m,n]hexes may have important electronic or optical properties. One could indeed wrap the spirographene sheet back onto itself and create spirographene cylinders analogous to the graphene cylinders seen in nanotubes.

In fully 3-dimensions one has the synthetic metal glitter, evidently there is no 3-dimensional analog to glitter in ordinary quantum chemistry, which extends to 2-D graphene sheets and no further. Glitter, as a synthetic metal, is already interesting from the point of view of its undoped metallic status. That its metallic state can be so tightly linked to the endo-spiroconjugation in it is also remarkable. One could envision fragments of the glitter lattice, analogous to the recently reported diamondoid hydrocarbon fragments of the diamond lattice, called the glitter[m,n,o]enes in which the indexes indicate the numbers of spiro nodes in the fragment along its length, width and height.

Clearly there is a rich area of research accessible to organic chemists, theorists, materials scientists and biologists in spiro quantum chemistry, and the results in this paper are only the beginning. Each class of spiro analogs to the ordinary hydrocarbons of quantum chemistry presents its own, unique synthetic challenges to the organic chemistry community. And certainly there is a wealth of problems for theorists pointed out by this paper. The abundant literature on spiroconjugation, alluded to in [7], suggests its importance in chemistry, biology, materials science and fundamental theory. It is hoped that chemists may be interested enough by the prospects of this manuscript to take up the cause of elucidating the fundamental features of spiro quantum chemistry.

Acknowledgments

One of us (M.J.B.) thank Professor Roald Hoffmann for his suggestions for writing this paper. I also thank Jane Jorgensen for her expert drawings. J.E.E. is thanked for giving me certain piece of mind through the teaching of aesthetic principles, some now written in stone, from which this research paper developed. I thank my wife Hsi-cheng Shen for her love and patience.

References

[1] M.J. Bucknum and R. Hoffmann, J. Am. Chem. Soc. 116 (1994) 11456.

[2] (a) L.A. Carreira, R.O. Carter and J.R. Durig, J. Chem. Phys. 59, 812 (1973) (b) H. Oberhammer and S.H. Bauer, J. Am. Chem. Soc., 91 (1969) 10. The structural information is based upon electron diffraction data of the gaseous 1,4-cyclohexadiene molecule. Carreira et al. report the ring in a planar equilibrium conformation.

[3] A.F. Wells, The Geometrical Basis of Crystal Chemistry: (a) Part 1, A.F. Wells, Acta Cryst. 7 (1954) 535. (b) Part 2, A.F. Wells, Acta Cryst. 7 (1954) 545. (c) Part 3, A.F. Wells, Acta Cryst. 7 (1954) 842. (d) Part 4, A.F. Wells, Acta Cryst. 7 (1954) 849. (e) Part 5, A.F. Wells, Acta Cryst. 8 (1955) 32. (f) Part 6, A.F. Wells, Acta Cryst. 9 (1956) 23. (g) Part 7, A.F. Wells and R.R. Sharpe, Acta Cryst. 16 (1963) 857. (h) Part 8, A.F. Wells, Acta Cryst. 18 (1965) 894. (i) Part 9, A.F. Wells, Acta Cryst. B24 (1968) 50. (j) Part 10, A.F. Wells, Acta Cryst. B25 (1969) 1711. (k) Part 11, A.F. Wells, Acta Cryst. B28 (1972) 711. (l) Part 12, A.F. Wells, Acta Cryst. B32 (1976) 2619. (m) A.F. Wells, *Three Dimensional Nets and Polyhedra*, 1st ed. (Wiley, New

York, 1977). (n) A.F. Wells, *Further Studies of Three-dimensional Nets*, American Crystallographic Association, Monograph #8, 1st ed. (ACA Press, 1979).
[4] K.M. Merz, R. Hoffmann and A.T. Balaban, J. Am. Chem. Soc. 109 (1987) 6742.
[5] (a) R. Hoffmann, J. Chem. Phys. 39 (1963) 1397. (b) R. Hoffmann and W.N. Lipscomb, J. Chem. Phys. 37 (1962) 2872. (c) M-H. Whangbo and R. Hoffmann, J. Am. Chem. Soc. 100 (1978) 6093. (d) M-H. Whangbo, R, Hoffmann and R.B. Woodward, Proc. Royal Soc. A366 (1979) 23.
[6] (a) H.E. Simmons and T. Fukunaga, J. Am. Chem. Soc. 89 (1967) 5208. (b) R. Hoffmann, A. Imamura and G. Zeiss, J. Am. Chem. Soc. 89 (1967) 5215.
[7] (a) V. Galasso, Chem. Phys. 153 (1991) 13. (b) S. Smolinski, M. Balazy, H. Iwamura, T. Sugawara, Y. Kawada and M. Iwamura, Bull. Chem. Soc. Jpn. 55 (1982) 1106. (c) H. Duerr and R. Gleiter, Angew. Chem. Int. Ed. Engli. 17 (1978) 559. (d) B.Y. Simkin, S.P. Makarov, N.G. Furmanova, K.S. Karaev and V.I. Minkin, Chem. Heteroc. Comp. 1 (1978) 948. (e) J.S. Foos, "Synthesis and Reactivity of Spiro[4.4]nonatetraene and Spiro[4.4]nona-1,3,6-triene", PhD thesis, (Cornell University, 1974). (f) C. Batich, E. Hielbronner, E. Rommel, M.F. Semmelhack and J.S. Foos, J. Am. Chem. Soc. 96 (1974) 7662. (g) R. Sustmann and R. Schubert, Angew. Chem. Int. Ed. Engl. 11 840, (1972). (h) H. Duerr and H. Kober, Justus Liebigs Ann. Chem. 740 (1970) 74. (i) E.W. Garbisch, Jr. and R.F. Sprecher, J. Am. Chem. Soc. 88 (1966) 3433. (j) P.E. Eaton and R.A. Hudson, J. Am. Chem. Soc. 87(1965) 2769. (k) K.N. Houk, J. Am. Chem. Soc. 87 (1965) 2769.
[8] V.I. Minkin, M.N. Glukhovtsev and B.Y. Simkin, *Aromaticity and Antiaromaticity: Electronic and Structural Aspects*, (Wiley, NY, 1994).
[9] A.F. Wells, *Structural Inorganic Chemistry*, (Oxford University Press, Oxford, UK, 1984).
[10] J.K. Williams and R.E. Benson, J. Am. Chem. Soc. 84 (1962) 1257.
[11] R.E. Benson and R.V. Lindsey, Jr., J. Am. Chem. Soc. 81 (1959) 4247.
[12] R.B. Woodward and R. Hoffmann, *The Conservation of Orbital Symmetry*, (Verlag Chemie, GmbH, Weinheim/Bergstrasse, 1970).
[13] (a) J. Donohue, *The Structure of the Elements*, (Wiley, NY, 1974). (b) W. Kraetschmer and H. Huffmann, Nature 347 (1990) 354. (c) H. Kroto, J.R. Heath, S.C. O'Brien, R.F. Curl and R.E. Smalley, Nature 318 (1985) 162. (d) E. Osawa, Kagaku 25 (1970) 85. (e) F.P. Bundy and J.S. Kasper, J. Chem. Phys. 46 (1967) 3437. (f) R.B. Aust and H.G. Drickamer, Science 140(1963) 817. (g) L. Zeger and E.Kaxiras, Phys. Rev. Lett. 70 (1993) 2929. (h) D.A. Muller, Y. Zhou, R. Raj, and J. Silcox, Nature 366 (1993) 725. (i) H. Hiura, T.W. Ebbensen, J. Fujita, K. Tanigaki and T. Takada, Nature 367(1994) 148. (j) C.L. Renschler, J. Pouch and D.M. Cox, (ed.) *Novel Forms of Carbon, MRS Symposium Proceedings*, 270 (MRS, Pittsburgh, 1992). (k) F. Moshary, N.H. Chen, I.F. Silvera, C.A. Brown, H.C. Dorn, M.S. de Vries and D.S. Bethune, Phys. Rev. Lett. 69 (1992) 466. (l) S. Iijima, Nature 354 (1991) 56. (m) W. Utsumi and T. Yagi, Science 252 (1991) 1542. (n) H. Hirai and K. Kondo, Science 253 (1991) 772. (o) K.E. Spear, A.W. Phelps and W.B. White, J. Mat. Res. 5 (1990) 2277. (p) A.V. Baitin, A.A. Lebedev, S.V. Romanenko, V.N. Senchenko and M.A. Scheindlin, High Temp.-High Press. 21 (1990) 157. (q) J.C. Angus and C.C. Hayman, Science 241 (1988) 913. (r) V.M. Melnitchenko, Y.N. Nikulin and A.M. Sladkov, Carbon 23 (1985) 3. (s) I.V. Stankevich, M.V. Nikerov and D.A. Bochvar, Russ. Chem. Rev. 53 (1984) 640. (t) A.G. Whittaker, E.J. Watts, R.S. Lewis and E. Anders Science 209 (1980) 1512. (u) A.G. Whittaker and B. Tooper, J. Am. Ceramic Soc. 57 (1974) 443. (v) D.A. Bochvar and E.G. Galpern, Dokl. Akad. Nauk. SSSR 209 (1973) 612. (w) A. El Gorsey and G. Donnay, Science 161 (1968) 363. (x) S. Ergun, Carbon 6 (1968) 141. (y) H. Drickamer, Science 156 (1967) 1183. (z) F.P. Bundy, J. Chem. Phys. 38 (1963) 631.
[14] R.M. Hazen, *The New Alchemists*, (Times Books-Random House, New York, 1994).
[15] P.W. Atkins, *Physical Chemistry*, 4th ed. (W.H. Freeman and Company, New York, 1990).

[16] More descriptive topological indexes are sometimes used in place of Schlaefli symbols because of the need to further identify nets with the same Schlaefli symbol (n, p). For example the graphite net has the index (6, 3), which is also the index for the square-octagon plane tiling and the pentagon-heptagon plane tiling.
[17] L. Euler, *Elementa Doctrinae Solidorum and Demonstratium Nonannularum in Signium Proprietatum Quibus Solid Heddris Planis Inclusas Unt Praedita*, included in the Proceedings of the St. Petersburg Academy, 1758.
[18] Explicit Euler equations for 3-, 4- and 5-connected polyhedra elegantly show the existence of the 5 regular convex polyhedra and the semi-regular Archimedean polyhedra.
[19] For 1-dimension, n and p can be viewed as each being equal to 2. (2, 2) has a number of edges, E, equal to 2. For n-sided polygons, the Schlaefli symbol is (n, 2) and the number of edges, E, is properly equal to n.
[20] A.F. Wells, in: *The Geometrical Basis of Crystal Chemistry: Part 7*, eds. A.F. Wells and R.R. Sharpe, Acta Cryst. 16 (1963) 857. This paper reports on a modification of the Euler relation for application to 3-dimensional polyhedra. Such polyhedra are infinite in extent and are represented by the Schlaefli symbols (3, n) where n is greater than 6, and other Schlaefli symbols, some of which are identical to those of the ordinary 3-dimensional nets.
[21] M. Wenninger, *Dual Models*, 1st ed. (Cambridge University Press, Cambridge, UK, 1983). And the references therein.
[22] A.F. Wells, *Further Studies of Three-dimensional Nets*, ACA Monograph #8, 1st ed. (ACA Press, 1979). And the references therein. Much previously unpublished material, concerned mainly with the vast topological subspace of 3-,4-connected networks, was reported in this publication. Scores of previously unknown structures, perhaps numbering more than 100, were reported. The explicit identification of structures with both fractional polygonality and fractional connectivity was made, anticipating much later work in various fields. These Wellsean structures are innumerable and their polyhedral analogs have recently been identified.
[23] W.L. Bragg and W.H. Zachariasen, Zeits. fur Kristoll. 72 (1930) 518.
[24] W.L. Bragg, *Atomic Structure of Minerals*, (Cornell University Press, Ithaca, NY, 1937).
[25] (a) R. Juza and H. Hahn, Naturwissenschaften 27 (1939) 32. (b) R. Juza and H. Hahn, Zeits. Anorg. Chem. 244 (1940) 125.
[26] D. Hardie and K.H. Jack, Nature 180 (1957) 332.
[27] S.N. Ruddleson and P. Popper, Acta Cryst. 11 465 (1958).
[28] M.L. Cohen, Phys. Rev. B 32 (1985) 7988.
[29] J. Waser and E.D. McClanahan, J. Chem. Phys. 19 (1951) 413.